Textures in a chiral smectic liquid-crystal film

Stephen A. Langer and James P. Sethna
Laboratory of Atomic and Solid State Physics, Cornell University, Ithaca, New York 14853
(Received 10 March 1986)

Freely suspended liquid-crystal films of the smectic-I phase of HOBACPC [$R(-)$ hexyloxybenzylidene p'-amino-2-chloropropyl cinnamate] display distinctive stripe and droplet textures. We derive these patterns from a Landau expansion of the free energy using a vector order parameter. Strong pinning boundary conditions lead to boojums in the droplets and stable defect lines between the stripes. The boojum is a two-dimensional version of its namesake in superfluid ^{3}He-A. The surface defect in the boojum is expelled from the smectic-I droplet in order to lower the internal gradient energy, leaving a defect-free texture. The expulsion distance and the width of the stripes are calculated in terms of the elastic constants.

I. INTRODUCTION

Smectic liquid crystals, in which the molecules arrange themselves in parallel layers, can be drawn into stable freely suspended films only a few molecular layers thick.[1–4] In the tilted smectic phases, such as SmC and SmI, the molecular optical axis $\hat{\mathbf{n}}$ lies at an angle to the layer normal (see Fig. 1). The direction of the projection $\hat{\mathbf{c}}$ of the molecular axis in the plane of the film can be observed by polarized reflection microscopy. Basically, if the direction of polarization of incident light is parallel or perpendicular to $\hat{\mathbf{c}}$, then the polarization is unchanged upon reflection, whereas if the direction of polarization of the incident beam is at some other angle, the polarization is rotated. When viewed through crossed polarizers, those regions of the film with $\hat{\mathbf{c}}$ parallel to either of the polarizers appear dark. These dark fringes are known as *schlieren* lines.[5] Defects in the liquid crystal show up as discontinuities or points of convergence of *schlieren* lines.

Distinctive *schlieren* patterns have been observed by Clark, Van Winkle, and Muzny[6] in freely suspended films of HOBACPC [$R(-)$ hexyloxybenzylidene p'-amino-2-chloropropyl cinnamate], a chiral liquid crystal which forms ferroelectric phases of SmC and SmI. Both SmC and SmI are tilted phases; while the nature of the ordering in these phases is still under investigation,[7] SmC is known to have only short-range positional order within layers, while SmI has a more pronounced hexagonal order and more translational order than does SmC. In both cases there exists orientational order between layers. On cooling a SmC film through 55 C small roughly circular domains of SmI nucleate. The SmI droplets drift away from their nucleation sites and grow into the SmC. The droplets are characterized by from one to three straight *schlieren* lines which appear to originate at a point off the edge of the droplet. (See Fig. 2.) The *schlieren* lines lie at 45° to one another. In circular droplets, relatively free from the distortions caused by contact with neighboring

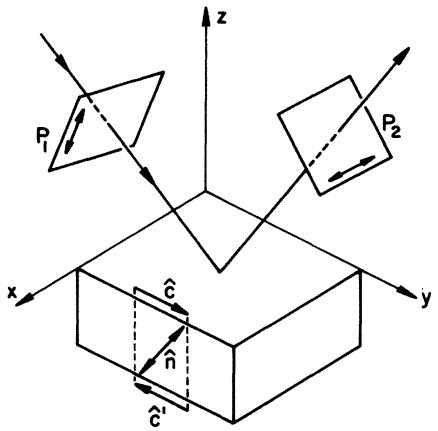

FIG. 1. Schematic of the experiment. The smectic film lies in the x-y plane. The film is viewed by reflection between crossed polarizers P_1 and P_2. The molecular optical axis is $\hat{\mathbf{n}}$—the molecule shown lies in the y-z plane. The order parameter $\hat{\mathbf{c}}$ points towards the tops of the tilted molecules, and lies in the x-y plane. Consequently, when the film is viewed from below, the order parameter $\hat{\mathbf{c}}'$ is the reverse of $\hat{\mathbf{c}}$.

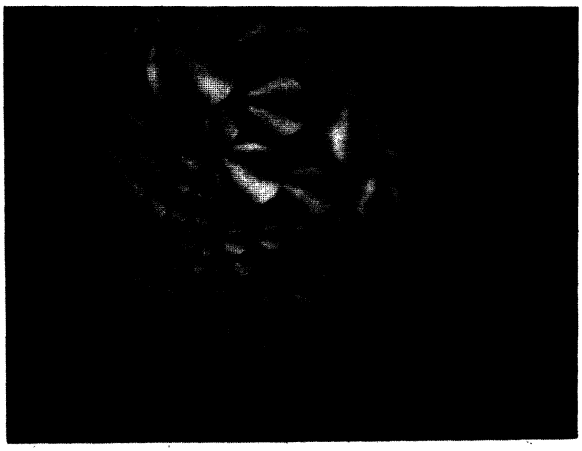

FIG. 2. Polarized reflection micrograph of the droplet texture. The polarization axes are parallel to the edges of the picture. The diameter of the illuminated region is roughly 0.24 cm. Photo courtesy of N. A. Clark, D. H. Van Winkle, and C. Muzny.

droplets, the schlieren lines terminate where the droplet boundary is parallel to one of the polarizers, indicating that $\hat{c}$ is either parallel or perpendicular to the boundary. Defects never appear inside the droplets.

As the drops grow they merge with one another, forming a striped pattern. (See Fig. 3.) The *schlieren* lines indicate that the optical axis is parallel to the edge of the stripe along the edge. Moving across the stripe, the optical axis rotates through 180° until it is parallel to the opposite edge of the stripe. At this point there is a defect line at which the optical axis reverses itself and a new stripe begins. The direction of rotation across a stripe is always the same.

If the same experiment is performed using a racemic mixture of HOBACPC (equal numbers of right- and left-handed molecules) the texture within the droplets is uniform, with no converging *schlieren* lines. The presence of the stripe and droplet patterns in the chiral case and the absence of the patterns in the racemic case can be explained by exploiting the different symmetries of the two systems. de Gennes[8] has suggested that a tilted smectic in three dimensions might exhibit a finite density of defects due to the chirality of the molecules. The tilted HOBACPC film is a two-dimensional realization of this prediction. In the body of this paper we write down the most general free energy for a tilted chiral smectic film and show how it leads to the stripe and droplet defect textures.

A. Conclusions

We describe the smectic film by a unit vector order parameter $\hat{c}$. There are two contributions to the free energy of the film—bulk terms involving integrals of gradients of $\hat{c}$ over the area of the system, and surface terms involving line integrals around the boundary of the system. In a system of size R the gradients of the order parameter scale as $1/R$. Since the bulk free-energy density is quadratic in the gradients, the total bulk free energy (integrated over the area of the sample) scales independently of R. On the other hand, the surface free energy per unit length is independent of the system size, so the total surface free energy scales as R. Hence, for large systems, where R is much greater than the molecular length, the surface energy dominates the bulk energy. Strong surface energies imply a strongly preferred angle between $\hat{c}$ and the boundary. These strong pinning boundary conditions are crucial in determining the patterns that the film can display.

The unusual symmetries of the chiral tilted smectic film allow the boundary conditions to take an unusual form. The order parameter at the perimeter of a region can prefer to point counterclockwise rather than clockwise, or vice versa. The assumptions that the SmI droplets are perfectly circular (due to the surface tension of the SmC-SmI interface) and that $\hat{c}$ lies parallel to the interface lead to the minimum-energy droplet texture shown in Fig. 4(a). The order parameter is continuous everywhere except at a defect at some point on the circumference. To find the orientation of $\hat{c}$ at a point in the interior, draw a straight line from the defect through the point in question. The orientation of $\hat{c}$ at the intersection of this line with the boundary is the orientation of $\hat{c}$ at the interior point. This construction satisfies the boundary conditions, produces straight *schlieren* lines, and minimizes the free energy. Most importantly, since the defect lies on the circumference, it can be expelled from the droplet at a small cost in surface energy but a great savings in bulk gradient energy. In Sec. III B we show that this pattern is indeed a minimum of the free energy and calculate how far the defect is expelled from the droplet.

The strong boundary conditions are also responsible for the presence of stripes in the film. Each defect-line core carries a positive free energy J_0 per unit length, but because the boundary condition can be satisfied along both sides of the defect lines, the net free energy of the lines may be negative. A negative defect energy does not lead to an infinite density of defect lines, however. In order to satisfy the boundary condition at both sides of a stripe, the order parameter must rotate through 180° between defect lines, so narrow stripes entail large gradient energies. The balance between gradient energies, surface energies, and defect core energies leads to a finite nonzero stripe width. This width is calculated in Sec. III A.

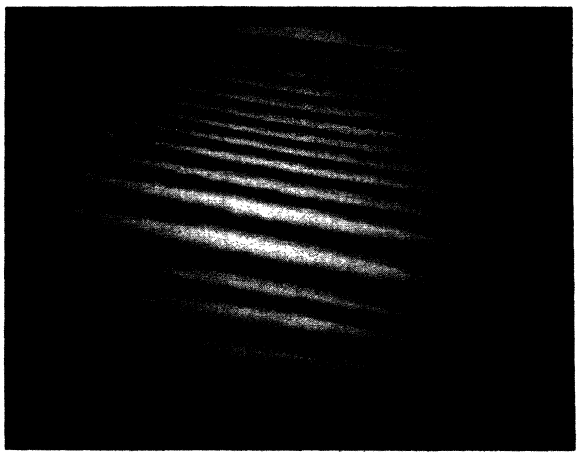

FIG. 3. Polarized reflection micrograph of the stripe texture. Photo courtesy of N. A. Clark, D. H. Van Winkle, and C. Muzny.

II. FORM OF THE FREE ENERGY

A. The order parameter

Let the smectic film lie in the x-y plane. At each point (x,y) in the film denote the local molecular axis of optical anisotropy by $\hat{n}$, averaged over thermal motions and the depth of the film. It is convenient to visualize $\hat{n}$ as the long axis of the molecules, although this does not necessarily coincide with the optical anisotropy axis. Assuming that the molecules are effectively symmetrical head to tail, there is no distinction between $\hat{n}$ and $-\hat{n}$, so $\hat{n}$ is a director rather than a vector. We will describe the film by a unit-vector order parameter $\hat{c}(x,y)$, or, equivalently, by an angle $\phi(x,y)$, where $\hat{c}=\hat{x}\cos\phi+\hat{y}\sin\phi$. $\hat{c}$ points along the projection of $\hat{n}$ in the x-y plane, as shown in Fig. 1.

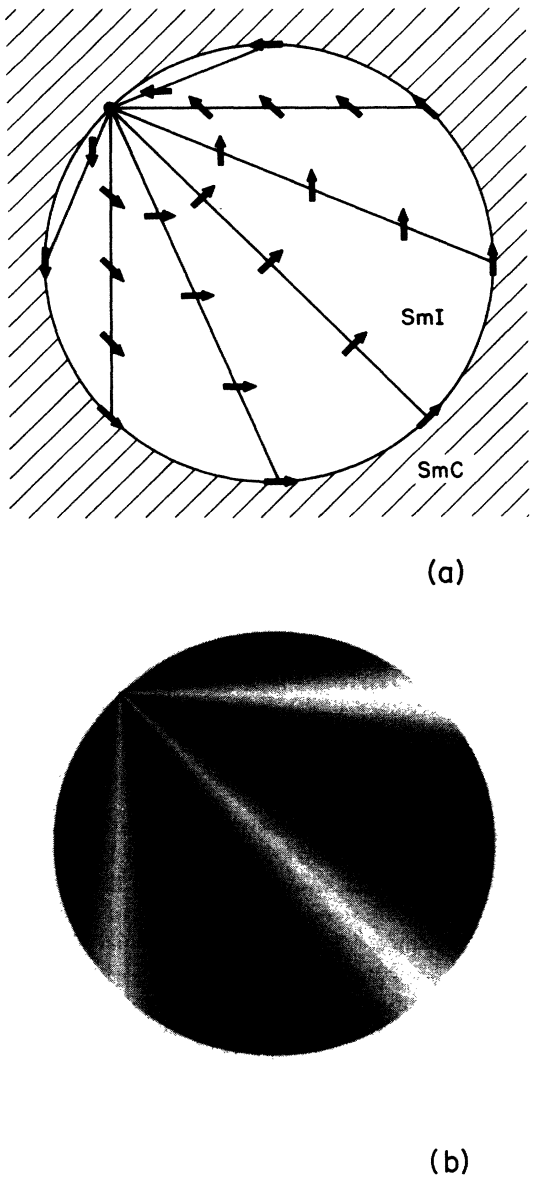

FIG. 4. (a) Texture within an ideal droplet. The order parameter is everywhere parallel to the boundary at the boundary, and the orientation of the order parameter is constant along any straight line passing through the defect point. (b) Computer-generated *schlieren* pattern for the configuration of (a).

Because rotating a tilted molecule by 180° around the $\hat{z}$ axis (perpendicular to the film) does not return it to its original configuration, $\hat{c}$, unlike $\hat{n}$, is a true vector. We define the head of the vector to point towards the end of the molecule lying near the top of the film.

Our order parameter does not contain any information about the translational order of the smectic phases. In particular, the order parameter cannot distinguish between SmI and SmC, and hence our theory does not describe the SmC-SmI transition. The theory requires at least three elastic constants and ascribes the differences between SmC and SmI to differences in these constants rather than variations in the magnitude or form of the order parameter.

HOBACPC has ferroelectric order, which in principle leads to nonlocal terms in the free energy. Pindak *et al.* found experimentally that they could neglect long-range dipole interactions in DOBAMBC (*p*-decyloxybenzylidene-*p'*-amino-2-methylbutylcinnamate), a material similar to HOBACPC, due to the presence of screening ionic impurities. Although the dipole moment of HOBACPC is stronger than that of DOBAMBC, we will also neglect these long-range forces.[3]

B. Symmetries of the free energy

The free energy of the film is

$$\mathcal{F}[\hat{c}]=\int\int dx\,dy F(\hat{c}(x,y))+\mathcal{F}_{\text{defect}} \tag{1}$$

where $\mathcal{F}_{\text{defect}}$ is the free energy of defect cores. The free-energy density F is a scalar function of $\hat{c}$ and its gradients, and must be invariant under all coordinate transformations which leave the x-y plane fixed. These include rotations about the $\hat{z}$ axis, rotations by 180° about the $\hat{x}$ or $\hat{y}$ axes, and translations in the $\hat{x}$ or $\hat{y}$ directions. Chiral molecules are not invariant under reflections, so if and only if the liquid crystal is racemic, F must be invariant under reflections through the x-y plane.

The free-energy density F can be decomposed into bulk and surface terms.[9] Bulk terms contribute to the total free energy over the whole area of the sample, but total divergences and other surface terms contribute only at boundaries and defects.

1. Bulk terms

The bulk gradient free-energy density is given by all those terms in a Landau expansion which are not total divergences and are compatible with the symmetries of the system. A simple scaling argument shows that the series may be truncated at second order in the derivatives of $\hat{c}$. Consider an nth-order term. The derivatives are of order R^{-n}, where R is the system size. The area integral in (1) contributes a factor of order R^2. The complete term has the dimensions of energy, so the elastic constant which multiples it must have dimensions of (energy)$\times$(length)$^{n-2}$. The only length which can come into the prefactor is the molecular size a, so the nth-order term scales as $(a/R)^{n-2}$. For systems large compared to the molecular size, high-order terms can be neglected in the bulk free energy.

For the system to be stable and have finite gradients in the bulk, it is necessary to retain terms up to at least second order. The only allowed nonzero zeroth-order term, $\hat{c}\cdot\hat{c}=1$, is constant and uninteresting. The first-order terms are all total divergences and will be treated later. Hence, the bulk free-energy density is composed solely of second-order terms.

The most general second-order term, not including total divergences, is

$$F_2=T_{ijkl}(\partial_i c_j)(\partial_k c_l)\ . \tag{2}$$

[Terms of the form $c_j(\partial_i\partial_k c_l)$ need not be considered because $\partial_i(c_j\partial_k c_l)=(\partial_i c_j)(\partial_k c_l)+c_j(\partial_i\partial_k c_l)$ is a total divergence. $T_{ijkl}c_j(\partial_i\partial_k c_l)$ is therefore equivalent to (2) as a

bulk term.] T_{ijkl} must be symmetric under the simultaneous interchange of i and j with k and l. As shown in Appendix A, there are only four linearly independent tensors of this sort invariant under rotations about $\hat{\mathbf{z}}$, leading to the following four terms in the free energy:

$$F_2^1 = K_s(\partial\cdot\hat{\mathbf{c}})^2 , \tag{3a}$$

$$F_2^2 = K_b(\partial\times\hat{\mathbf{c}})^2 , \tag{3b}$$

$$F_2^3 = K_3(\partial\cdot\hat{\mathbf{c}})(\partial\times\hat{\mathbf{c}}) , \tag{3c}$$

$$F_2^4 = K_4(\partial_i c_j)^2 . \tag{3d}$$

Note that in two dimensions $\partial\times\hat{\mathbf{c}}=\varepsilon_{ij}\partial_i c_j$ is a scalar. ε_{ij} is the antisymmetric tensor of rank two. $\varepsilon_{12}=-\varepsilon_{21}=1$; $\varepsilon_{11}=\varepsilon_{22}=0$.

Requiring symmetry under 180° rotations about the $\hat{\mathbf{x}}$ axis eliminates the third term. Under such a rotation, $\hat{\mathbf{c}}$ is transformed to $\hat{\mathbf{c}}'$ (see Fig. 5), where

$$c_x' = -c_x(x,-y) \tag{4a}$$

and

$$c_y' = c_y(x,-y) . \tag{4b}$$

This follows from the definition of $\hat{\mathbf{c}}$—$\hat{\mathbf{c}}$ points toward the top end of the molecule, so when the film is turned over, $\hat{\mathbf{c}}$ points towards the other end. Furthermore, c_y reverses upon rotation about $\hat{\mathbf{x}}$, leading immediately to Eq. (4).

Because $d/dx' = d/dx$ and $d/dy' = -d/dy$, we have

$$\partial'\cdot\hat{\mathbf{c}}' = -\partial\cdot\hat{\mathbf{c}} \tag{5a}$$

and

$$\partial'\times\hat{\mathbf{c}}' = \partial\times\hat{\mathbf{c}} . \tag{5b}$$

Therefore F cannot contain terms odd in $\partial\cdot\hat{\mathbf{c}}$, and K_3 must be zero.

Since $\hat{\mathbf{c}}$ is a unit vector,

$$(\partial_i c_j)^2 = (\partial\cdot\hat{\mathbf{c}})^2 + (\partial\times\hat{\mathbf{c}})^2 , \tag{6}$$

so F_2^4 is not independent of F_2^1 and F_2^2. Hence the gradient free energy is simply given by

$$F_2 = K_s(\partial\cdot\hat{\mathbf{c}})^2 + K_b(\partial\times\hat{\mathbf{c}})^2 . \tag{7}$$

K_s gives the energy due to splaying the order-parameter field, and K_b gives the energy due to bending. It will be useful to redefine K_s and K_b in terms of

$$K = K_s + K_b \tag{8}$$

and

$$\beta = \frac{K_s - K_b}{K_s + K_b} \tag{9}$$

so that

$$F_2 = \tfrac{1}{2}K(1+\beta)(\partial\cdot\hat{\mathbf{c}})^2 + \tfrac{1}{2}K(1-\beta)(\partial\times\hat{\mathbf{c}})^2 . \tag{10}$$

The free-energy density (10) must have a minimum for finite $\partial\cdot\hat{\mathbf{c}}$ and $\partial\times\hat{\mathbf{c}}$. Hence, K_s and K_b must be positive, so $K>0$ and $|\beta|\le 1$.

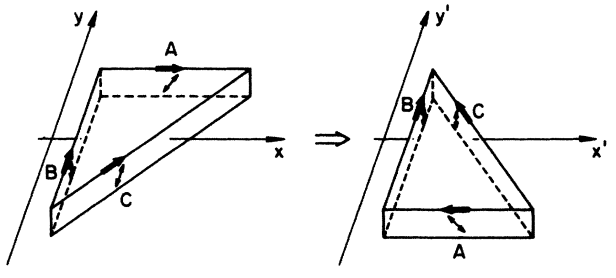

FIG. 5. Transformation of the order parameter under a 180° rotation about $\hat{\mathbf{x}}$. The x components of the in-plane projections of the molecular axes are reversed on rotation, but the y components are not.

2. *Surface terms*

Total divergences in the Landau expansion of F are terms of the form $\partial\cdot[\hat{\mathbf{c}}g(\hat{\mathbf{c}})]$ and $\partial\times[\hat{\mathbf{c}}g(\hat{\mathbf{c}})]$ where $g(\hat{\mathbf{c}})$ is any scalar function of $\hat{\mathbf{c}}$ and its derivatives. These terms are surface terms because

$$\int\int dx\,dy\,\partial\cdot[\hat{\mathbf{c}}g(\hat{\mathbf{c}})] = \oint g(\hat{\mathbf{c}})\hat{\mathbf{c}}\times dl \tag{11a}$$

and

$$\int\int dx\,dy\,\partial\times[\hat{\mathbf{c}}g(\hat{\mathbf{c}})] = \oint g(\hat{\mathbf{c}})\hat{\mathbf{c}}\cdot dl . \tag{11b}$$

The path of integration encloses all regions of the film where $\hat{\mathbf{c}}$ is continuous and differentiable. However, since not all of the allowed surface terms can be expressed as area integrals of total divergences, we must consider in general the line integral of a surface free-energy density.

As shown in Appendix B, the surface free-energy density cannot depend on derivatives of the order parameter normal to the boundary, and the lowest-order nonvanishing tangential derivatives are of higher order than F_2. Hence, we can write the net surface free energy as

$$\mathcal{F}_{\rm surf} = \oint F_{\rm surf}(\hat{\mathbf{c}}\cdot\hat{\mathbf{n}},\hat{\mathbf{c}}\times\hat{\mathbf{n}})dl , \tag{12}$$

where $\hat{\mathbf{n}}$ is the unit normal to the surface. As usual, $F_{\rm surf}$ must be invariant under rotation by 180° about the $\hat{\mathbf{x}}$ axis. This rotation maps $\hat{\mathbf{c}}\cdot\hat{\mathbf{n}}\to-\hat{\mathbf{c}}\cdot\hat{\mathbf{n}}$ and $\hat{\mathbf{c}}\times\hat{\mathbf{n}}\to\hat{\mathbf{c}}\times\hat{\mathbf{n}}$. Hence $F_{\rm surf}$ must depend quadratically on $\hat{\mathbf{c}}\cdot\hat{\mathbf{n}}$. Because $(\hat{\mathbf{c}}\cdot\hat{\mathbf{n}})^2 = 1-(\hat{\mathbf{c}}\times\hat{\mathbf{n}})^2$, $F_{\rm surf}$ depends on $\hat{\mathbf{c}}\times\hat{\mathbf{n}}$ alone. For chiral systems with no reflection symmetry

$$\mathcal{F}_{\rm surf} = \oint F_{\rm surf}(\hat{\mathbf{c}}\times\hat{\mathbf{n}})dl . \tag{13}$$

In racemic mixtures $F_{\rm surf}$ must be invariant under reflections, which requires quadratic dependence on $\hat{\mathbf{c}}\times\hat{\mathbf{n}}$ as well.

The absence of the stripe and droplet patterns in racemic mixtures indicates that the patterns are due to terms in the free energy forbidden by reflection symmetry. In Secs. III A and III B we will demonstrate that this is indeed the case. Assuming that the surface free energy is of the simplest form that differentiates between chiral and racemic mixtures, then

$$F_{\rm surf}(\hat{\mathbf{c}}\times\hat{\mathbf{n}}) = 2Kq\hat{\mathbf{c}}\times\hat{\mathbf{n}} . \tag{14}$$

The elastic constant q has dimensions of inverse length

and is a measure of the chirality of the system. For a racemic mixture $q=0$. If the angle between $\hat{c}$ and the boundary is θ, then q gives the strength of the θ^2 term in an expansion of $F_{\rm surf}$. In other words, for small θ, q behaves like a spring constant tending to restore tangential boundary conditions.

In principle $F_{\rm surf}$ can have a minimum at any value of $\hat{c}\times\hat{n}$, if higher-order terms are included in $F_{\rm surf}$. The assumption (14) is consistent with experiment—$\hat{c}\times\hat{n}$ is minimized when $\hat{c}$ is parallel to the boundary, and leads to antiparallel boundary conditions for the stripe pattern. We have no *a priori* explanation for the experimentally observed boundary conditions.

Equation (14) leads to the free energy

$$\mathcal{F}=\int\int dx\,dy\,F_2(\hat{c}(x,y))-2Kq\oint\hat{c}(x,y)\cdot dl+\mathcal{F}_{\rm defect} \tag{15}$$

with $F_2(\hat{c}(x,y))$ given by (10). The surface term in (15) scales linearly with the system size R. Since the second-order bulk gradient terms (10) scale independently of R, for large systems the surface energies dominate (strong pinning boundary conditions).

If β is near -1, then the total free energy may be written

$$\mathcal{F}\approx\int\int dx\,dy\,K(\partial\times\hat{c}-q)^2+\mathcal{F}_{\rm defect}+\text{const}\ , \tag{16}$$

where we have used Stokes Law to write the surface term as an area integral. This form of $\mathcal{F}$ suggests an alternate interpretation of the total divergence term, where q is not the strength of the boundary condition but rather a spontaneous bend in the bulk.

III. MINIMIZATION OF THE FREE ENERGY

A. Stripes

The details of the stripe pattern are determined by the competition between the bulk free energy F_2 and the surface free energy. The bulk energy is minimized by a uniform order parameter, but the boundary terms prefer $\hat{c}$ pointing in opposite directions on opposite sides of the stripe. Both conditions can be satisfied arbitrarily well in arbitrarily large stripes. However, if the cost of a defect line is not too great, the system prefers to gain bulk gradient energy and defect core energy in order to lose surface energy, and the stripes will have a finite width.

Essentially, the stripe pattern is one dimensional. We are mainly interested in the variation of $\hat{c}$ across the width of the stripe, so we assume that $\hat{c}$ is independent of position along the length of the stripe. We implicitly assume that the stripes are infinitely long. If the $\hat{y}$ axis points in the direction of the stripes (see Fig. 6) then all y derivatives vanish, and the bulk free-energy density (10) reduces to

$$F_2=\tfrac{1}{2}K\phi_x^2[1-\beta\cos(2\phi)]\ , \tag{17}$$

where $\hat{c}=\hat{x}\cos\phi+\hat{y}\sin\phi$ as usual, and $\phi_x\equiv\partial\phi/\partial x$. Given a width L and boundary conditions $\phi(0)=\phi_0$, $\phi(L)=\phi_1$, we find $\phi(x)$ by minimizing the bulk free energy per unit length of a single stripe,

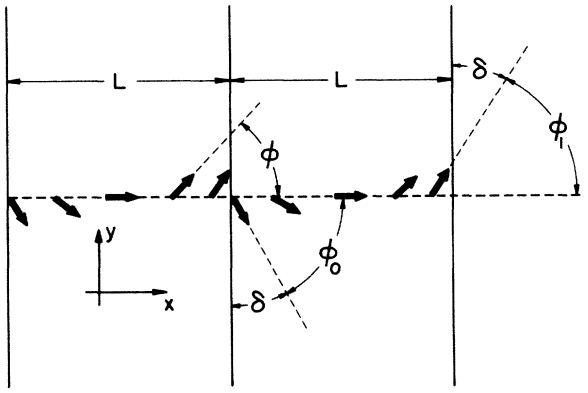

FIG. 6. Geometry of the stripe pattern, showing two stripes separated by a defect line. The order parameter $\hat{c}$ makes an angle $\phi(x)$ with the x axis. At the left-hand edge of a stripe $\phi=-\pi/2+\delta$, and at the right-hand edge $\phi=\pi/2-\delta$.

$$\tilde{\mathcal{F}}=\int_0^L F_2dx\ . \tag{18}$$

We then minimize $\tilde{\mathcal{F}}$ with respect to the boundary conditions, since $\hat{c}$ need not be exactly parallel to the sides of the stripe, and finally minimize the total free energy with respect to the stripe width. The end result is the stripe structure $\hat{c}(x)$ and the stripe width as functions of the elastic constants K, β, and q, and the defect core energy.

The Euler-Lagrange formula applied to (17) yields

$$\beta\sin(2\phi)\phi_x^2=[\beta\cos(2\phi)-1]\phi_{xx}\ , \tag{19}$$

which has the implicit solution

$$x-x_0=\frac{1}{Q}\int_{\phi(x_0)}^{\phi(x)}d\phi'\sqrt{1-\beta\cos(2\phi')}\ , \tag{20}$$

where Q is chosen so that $\phi(L)=\phi_1$. Substituting $\phi_x=Q[1-\beta\cos(2\phi)]^{-1/2}$ into (17) shows that the free-energy density across the stripe is independent of x,

$$F_2=\tfrac{1}{2}KQ^2=\frac{K}{2L^2}\left[\int_{\phi_0}^{\phi_1}d\phi\sqrt{1-\beta\cos(2\phi)}\right]^2\ , \tag{21}$$

so the bulk free energy per stripe per unit length $\tilde{\mathcal{F}}=LF_2$ is expressed in terms of the stripe width and the boundary conditions only.

The surface free energy per unit stripe length is, according to (15),

$$\tilde{\mathcal{F}}_{\rm surf}=-2Kq(\sin\phi_1-\sin\phi_0)\ . \tag{22}$$

In a system of total width L_0 there are L_0/L stripes and L_0/L defect lines between stripes, each with core energy J_0 per unit length. The total free energy of the system is

$$\mathcal{F}=\frac{L_0}{L}\left[\frac{K}{2L}f_\beta(\phi_0,\phi_1)-2Kq(\sin\phi_1-\sin\phi_0)+J_0\right]\ , \tag{23}$$

where

$$f_\beta(\phi_0,\phi_1)=\left[\int_{\phi_0}^{\phi_1}d\phi\sqrt{1-\beta\cos(2\phi)}\right]^2\ . \tag{24}$$

First, consider the limit of strong surface energies, $q \gg 1/L$. In this case the director is strictly parallel to the defect lines at the edges of the stripe, so

$$\mathcal{F} = \frac{L_0}{L}\left[\frac{K}{2L} f_\beta(-\pi/2,\pi/2) + J_0 - 4Kq\right] . \tag{25}$$

$\mathcal{F}$ is minimized for

$$L = \frac{f_\beta(-\pi/2,\pi/2)}{4q - J_0/K} . \tag{26}$$

Stripes do not occur (i.e., have infinite width) for $q < J_0/4K$.

When q is not large compared to $1/L$, the boundary angles ϕ_0 and ϕ_1 can relax to lower the bulk free energy. From (23) it follows that if $\phi_1 = \pi/2 - \delta$ is an equilibrium angle at the right edge of a strip of width L, then $\phi_0 = -\pi/2 + \delta$ is an equilibrium angle at the left edge. (See Fig. 6.) Define

$$I(\delta) = \int_{-\pi/2+\delta}^{\pi/2-\delta} d\phi \sqrt{1-\beta\cos(2\phi)} . \tag{27}$$

The bulk and surface free energy of a single stripe becomes

$$\mathcal{F}_0(\delta,L) = \frac{K}{2L}[I(\delta)]^2 - 4Kq\cos\delta . \tag{28}$$

The total free energy per unit length is

$$\mathcal{F} = \frac{L_0}{L}(\mathcal{F}_0 + J_0) . \tag{29}$$

The equilibrium condition $\partial\mathcal{F}_0/\partial\delta = 0$ yields a relationship between strip length and edge angle,

$$qL = \frac{\sqrt{1+\beta\cos(2\delta)}}{2\sin\delta} I(\delta) . \tag{30}$$

In principle, L and δ can be measured experimentally, so (30) relates the elastic constants q and β. In practice, since δ is near zero, we can write

$$I(\delta) \approx I(0) - 2\delta\sqrt{1+\beta} + O(\delta^3) , \tag{31}$$

where

$$I(0) = \int_{-\pi/2}^{\pi/2} d\phi \sqrt{1-\beta\cos(2\phi)} , \tag{32}$$

so that

$$qL \approx \frac{I(0)\sqrt{1+\beta}}{2\delta} . \tag{33}$$

If $\beta \approx -1$, then (30) becomes

$$qL \approx \frac{1}{\sqrt{2}} I(\delta) \approx 2 \tag{34}$$

to lowest order in δ and $1+\beta$.

In general, to find δ in terms of the elastic constants we use (30) to eliminate L in (28), giving $\mathcal{F}_0$ as a function of δ,

$$\mathcal{F}_0(\delta) = Kq\left[\frac{\sin\delta\, I(\delta)}{\sqrt{1+\beta\cos(2\delta)}} - 4\cos\delta\right] . \tag{35}$$

Differentiating (29) with respect to δ and setting the result to zero gives an explicit equation for the equilibrium δ,

$$\frac{d\mathcal{F}_0}{d\delta} = \frac{\mathcal{F}_0(\delta) + J_0}{L(\delta)} \frac{dL}{d\delta} , \tag{36}$$

or, by using (30) and (35),

$$0 = h(\delta) = (1+\beta)\sin(2\delta) I(\delta) + 4\sin^2\delta[1+\beta\cos(2\delta)]^{3/2} + \left[\frac{J_0}{Kq} - 4\cos\delta\right]\left[(1+\beta)\cos\delta\sqrt{1+\beta\cos(2\delta)} + \frac{2\sin\delta[1+\beta\cos(2\delta)]^2}{I(\delta)}\right] . \tag{37}$$

We are interested in the zeros of $h(\delta)$ for $\delta > 0$, since $\delta < 0$ adds to the bulk free energy by increasing internal gradients of $\hat{\mathbf{c}}$. $(1+\beta)$ and $I(\delta)$ are non-negative, so the first two terms are non-negative. Hence, when $J_0 > 4Kq$ and the third term is positive, there are no zeros of h and stripes do not form. This result agrees with that previously obtained in the large-q limit. Figure 7 shows L and δ versus J_0/Kq for a variety of β's. Notice that $L \to 0$ and $\delta \to \pi/2$ as $J_0 \to 0$. When defect lines are free, the optimal configuration has an infinite density of defects and zero bulk gradient energy.

Since, for a given β, the stripe width and edge angle depend only on the ratio J_0/Kq, the large q limit corresponds to the small J_0 limit. At first glance this is a surprising result, implying that the boundary condition is violated more strongly ($\delta \to \pi/2$) as the strength of the surface term increases ($q \to \infty$). We can understand this result in either of two ways, depending on whether the chiral surface term (14) is incorporated into the bulk free energy, as in Eq. (16), or it is treated separately, as it has been so far. In the former case, the free-energy density across a stripe is not uniform, but is lower in the center than at the edges, leading to an effective attractive force between defect lines. In the latter case, the effective defect line tension is *negative,* and the free energy is lowest when there are a large number of narrow stripes.

When the surface free energy is treated separately from the bulk, then the effective defect-line tension, according to Eq. (37), is $J_0 - 4Kq\cos\delta$. For large enough q, δ can be arbitrarily close to $\pi/2$ while the line energy remains negative, and as long as the line energy is negative, it is beneficial for the system to increase the number of stripes. Hence, the stripe width vanishes and $\delta = \pi/2$ when the surface energy is infinitely strong.

On the other hand, when the surface terms are absorbed into the bulk terms in the free energy the line tension is always positive. Interpreted as a bulk term, the surface energy (14) contributes an amount $-2KqQ\cos\phi$

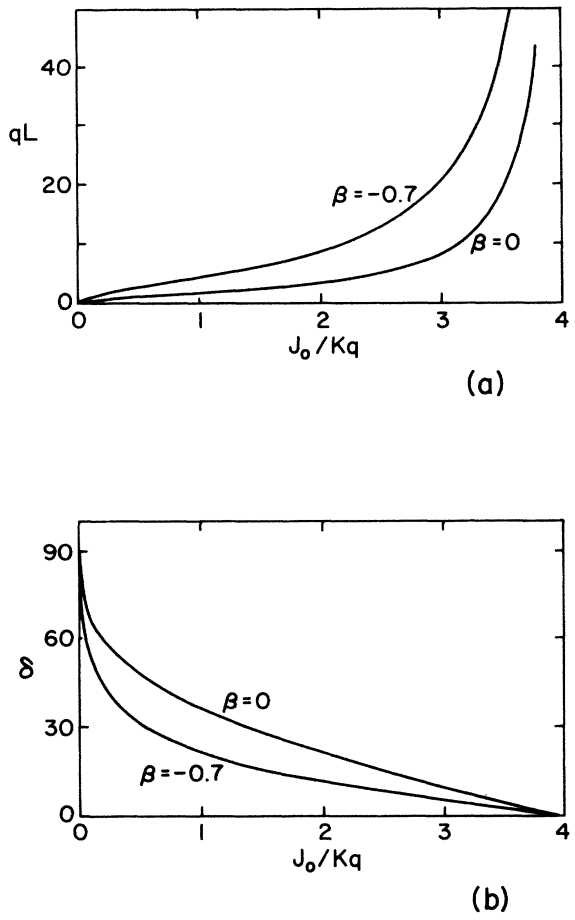

FIG. 7. (a) Stripe width L vs the reduced defect core energy J_0/Kq for $\beta=0$ and -0.7. L diverges when $J_0=4Kq$. (b) Stripe edge angle δ vs the reduced defect core energy J_0/Kq.

$\times(1-\beta\cos 2\phi)^{-1/2}$ to the bulk-energy density (21). This energy density is a minimum at the center of the stripe, where $\phi=0$. There is an effective attraction between defect lines because by moving the lines closer together [for a fixed $\phi(x)$] a larger fraction of the stripe is made up of the low-energy region in the center. As q increases, the attraction between lines increases, so the stripe width decreases, in agreement with Fig. 7.

In the racemic case, $q=0$, and the free energy (28) of a stripe is minimized when $I(\delta)=0$, or $\delta=\pi/2$. In other words, $\phi_0=\phi_1$ and the order parameter is uniform. Stripes do not occur in racemic mixtures.

In conclusion, two of the measurable characteristics of the stripe pattern are the width L and the angle δ between the order parameter and the stripe edge. We have calculated both of these quantities in terms of the elastic constants. The important quantities are β, the relative strength of the bulk splay and bend energies, and J_0/Kq, the ratio of the line defect core energy density to the strength of the bulk energies times the chirality.

B. Droplets

The fundamental difference between a droplet and a stripe is that the boundary of a droplet is a simple closed curve of finite extent, whereas the boundary of a stripe is infinite and open. If $\hat{c}$ is to be everywhere parallel to the boundary, then the topology of the droplet requires the presence of a defect either within (Fig. 8) or on the boundary of (Fig. 4) the droplet. For this reason, the droplet is a two-dimensional analog of the famous boojum[10] in superfluid ^{3}He-A. In ^{3}He-A the order parameter consists of a pair of orthonormal vectors $\vec{\phi}_1$ and $\vec{\phi}_2$. The normal to these vectors, $\vec{l}=\vec{\phi}_1\times\vec{\phi}_2$, is constrained to be perpendicular to the walls of the container. In a topologically spherical container, the flow lines of $\vec{l}$ must converge at some point. Vortex lines in the superfluid draw the point defect to the wall of the container, producing a boojum. In the smectic film the lines of $\hat{c}$ are perpendicular to the analogous lines of $\vec{l}$, and there are no vortices, but the resulting defect structure is qualitatively the same. Hu, Ham, and Saslow[11] have shown that the surfaces perpendicular to $\vec{l}$ in the ^{3}He-A boojum for a particular (and possibly unphysical) choice of a parameter κ are spheres passing through the defect point, just as the curves parallel to $\hat{c}$ in the smectic droplet are circles passing through the defect. The nested circles in Fig. 2 of Hu, Ham, and Saslow are cross sections of spheres, and are directly analogous to the nested circles in our Fig. 4. The essential fact is that in both cases a topological defect escapes to the boundary of the system.

The winding number s of a defect is the number of times that the order parameter $\hat{c}$ rotates through 2π along any closed path encircling the defect, independent of the chosen path. Consider an isolated droplet of SmI in a film of SmC. In the limit of large q (large chirality and strong boundary conditions), the surface term in (15) requires that $\hat{c}$ be parallel to the interface. $\hat{c}$ rotates through one complete revolution during one trip around the the boundary, so there must be a defect in the droplet. A solitary defect in the interior must have $s=1$. If the

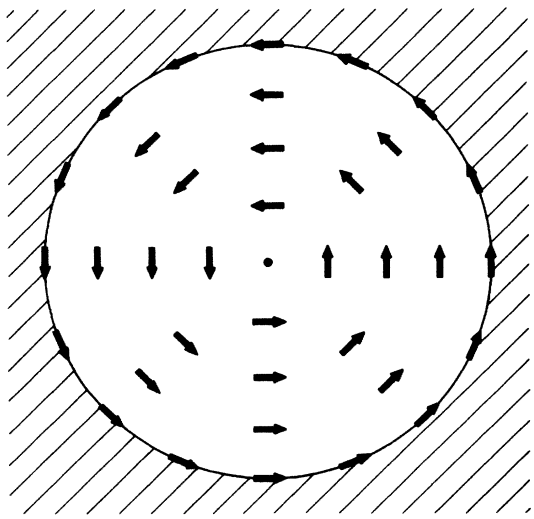

FIG. 8. Another method of filling a circular region with tangential boundary conditions. Unlike in Fig. 4(a), the defect here is trapped within the droplet and cannot escape without inducing large distortions in the texture.

defect lies on the boundary then the winding number is not fixed topologically, because no path can encircle the defect and remain within the SmI droplet.

On the other hand, if there is a natural way to extend the order parameter field to the exterior of the droplet, then we can consider the droplet to be a section of a pattern containing a defect with a well-defined winding number. If the boundary is smooth at the defect, then this winding number is 2 because $\hat{\mathbf{c}}$ rotates through one complete revolution upon traversing half a path (see Fig. 9). If the droplet is circular, then there is a particularly natural way to fill it with a section of an $s=2$ pattern. According to elementary geometry, an angle inscribed in a circle subtends an arc equal to twice the angle. Because of this fact, the $s=2$ pattern given by $\phi(\mathbf{r})=2\theta(\mathbf{r})+\pi/2$ has $\hat{\mathbf{c}}$ tangent to *any* circle centered on the $\hat{\mathbf{x}}$ axis and passing through the origin (see Fig. 10). Here $\theta(\mathbf{r})$ is the angle between $\mathbf{r}$ and $\hat{\mathbf{x}}$, and the defect sits at the origin. Since the surface tension of the SmC-SmI interface will make the SmI region circular, we expect the SmI droplets to follow this $s=2$ pattern.

Droplets formed of such a pattern have straight *schlieren* lines because ϕ is independent of r, in agreement with experiment. The *schlieren* lines lie at 45° to one another, also in agreement with experiment. Since, as shown below, the bulk free energy diverges logarithmically at a point defect, we expect the defect to be expelled from the droplet.[12] The resulting defect-free texture necessarily violates the boundary conditions at some point, but the cost in surface energy is bounded, whereas the cost of a point defect is not.

We now show that the proposed $s=2$ configuration is indeed predicted[13] by our model free energy for a chiral system, and compute roughly the defect expulsion distance d. The bulk free-energy density (10) in terms of ϕ is

$$F_2=\tfrac{1}{2}K\{\phi_x^2+\phi_y^2+\beta[(\phi_y^2-\phi_x^2)\cos(2\phi) -2\phi_x\phi_y\sin(2\phi)]\}\ . \tag{38}$$

The Euler-Lagrange formula in two dimensions

$$\frac{\partial F_2}{\partial\phi}-\frac{d}{dx}\frac{\partial F_2}{\partial\phi_x}-\frac{d}{dy}\frac{\partial F_2}{\partial\phi_y}=0 \tag{39}$$

applied to (38) yields

$$\phi_{xx}+\phi_{yy}+\beta[\sin(2\phi)(\phi_x^2-2\phi_{xy}-\phi_y^2) -\cos(2\phi)(\phi_{xx}+2\phi_x\phi_y-\phi_{yy})]=0\ . \tag{40}$$

Trying a solution of the form $\phi=s\theta+\phi_0$, and substituting

$$\phi_x=-\frac{s}{r}\sin\theta\ , \tag{41a}$$

$$\phi_y=\frac{s}{r}\cos\theta\ , \tag{41b}$$

$$\phi_{xx}=-\phi_{yy}=\frac{s}{r^2}\sin(2\theta)\ , \tag{41c}$$

and

$$\phi_{xy}=-\frac{s}{r^2}\cos(2\theta) \tag{41d}$$

into (40) gives

$$\frac{\beta}{r^2}(s^2-2s)\sin(2\theta-2\phi)=0\ . \tag{42}$$

The allowed winding numbers are therefore $s=0$ (uniform $\hat{\mathbf{c}}$, $\phi=\phi_0$), $s=1$ (radial $\hat{\mathbf{c}}$ with $\phi=\theta$, $\phi=\theta+\pi$; or tangential $\hat{\mathbf{c}}$, $\phi=\theta\pm\pi/2$), and $s=2$. Other winding numbers are allowed only if ϕ either does not depend linearly on θ or depends on r. (Note that the commonly used "one constant approximation," in which $K_s=K_b$ and $\beta=0$, al-

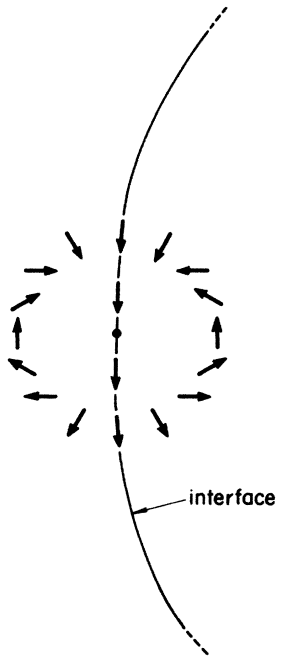

FIG. 9. An $s=2$ defect. ϕ rotates by 4π along any simple closed loop encircling the defect. If the defect lies on a smooth interface, then only half the loop exists. ϕ rotates by 2π along this half path, making ϕ continuous along the interface.

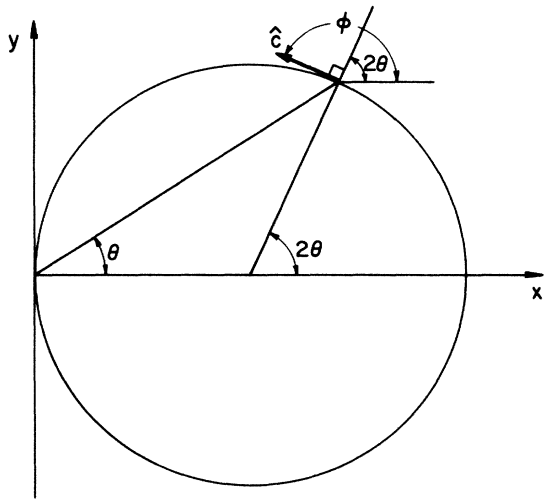

FIG. 10. Why $\phi=2\theta+\pi/2$ is a natural pattern for filling a circle with tangential boundary conditions.

lows *all* values of s and therefore should be used cautiously for general structural calculations.) Computation of the second variation of $\mathcal{F}$ shows that the $s=2$ solution is stable under small perturbations.

The bulk gradient free-energy density according to (38) is

$$F_2=\begin{cases}0 & (s=0)\\ \dfrac{K}{2r^2}[1+\beta\cos(2\phi_0)] & (s=1)\\ \dfrac{2K}{r^2}\{1+\beta\cos[2(\theta+\phi_0)]\} & (s=2)\,.\end{cases} \tag{43}$$

Integrating F_2 over an area including the origin produces a logarithmic divergence for $s=1$ and 2 as promised. In our model, if there are no boundary conditions ($q=0$) the uniform $s=0$ pattern is preferred, so racemic systems have texture-free droplets

We now compute the distance d at which the apparent defect sits outside the circular droplet of radius R for the case $\beta=-1$ and $\phi=2\theta+\pi/2$. We assume, without apology, that although the boundary conditions are no longer met exactly the SmI region remains circular and the interior pattern is not distorted. We also assume that the center of the circle lies on the x axis, at a distance $\rho=R+d$ from the apparent defect at the origin.

The bulk free energy is

$$\mathcal{F}_2=\int_0^R r'dr'\int_0^{2\pi}d\theta'4K\frac{\cos^2\theta}{r^2}\,, \tag{44}$$

where (r',θ') are the coordinates of a point relative to the center of the circle, and (r,θ) are the coordinates relative to the origin. (See Fig. 11.) Using the laws of sines and cosines to eliminate θ and r gives

$$\mathcal{F}_2=\int_0^R r'dr'\int_0^{2\pi}d\theta'\left[\frac{1}{r'^2+\rho^2+2r'\rho\cos\theta'}-\frac{r'^2\sin^2\theta'}{(r'^2+\rho^2+2r'\rho\cos\theta')^2}\right]. \tag{45}$$

The θ' integrals can be done by contour integration in $\zeta=e^{i\theta'}$, after which the r' integral is elementary. The result is that

$$\mathcal{F}_2=2\pi K\left\{\left[\frac{R}{\rho}\right]^2-\ln\left[1-\left[\frac{R}{\rho}\right]^2\right]\right\}. \tag{46}$$

The surface free energy is given by

$$\mathcal{F}_{\rm surf}=-2Kq\oint\hat{\mathbf{c}}\cdot d\mathbf{l}=-2Kq\int_0^{2\pi}R\,d\theta'\sin(\theta'-\phi)\,. \tag{47}$$

On substituting for ϕ in terms of θ' and integrating, we find that

$$\mathcal{F}_{\rm surf}=-4\pi Kq\frac{R^2}{\rho}\quad(R<\rho)\,. \tag{48}$$

The surface free energy is minimized by $\rho=R$; the bulk free energy is minimized by $\rho=\infty$. The equilibrium value

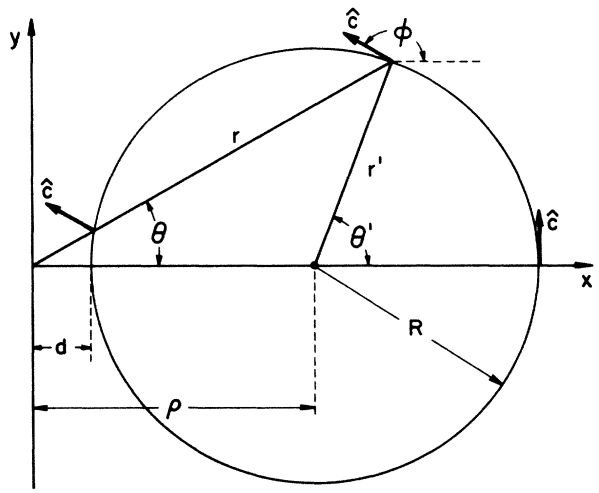

(a)

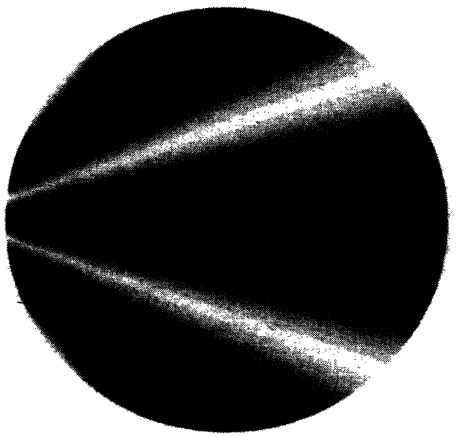

(b)

FIG. 11. (a) Geometry of the droplets. ϕ is a function only of θ. The droplet has moved a distance d relative to the defect. When $d=0$ the boundary conditions are met exactly, as in Fig. 4(a). (b) Computer generated *schlieren* pattern for the configuration of (a), with $d=R/4$.

of ρ is given by the minimum of

$$\mathcal{F}=2\pi K\left[\frac{R^2}{\rho^2}-\ln\left[1-\frac{R^2}{\rho^2}\right]-2q\frac{R^2}{\rho}\right], \tag{49}$$

which occurs when

$$\frac{2-R^2/\rho^2}{1-R^2/\rho^2}=q\rho\,. \tag{50}$$

Let $R=\rho(1+\Delta)$. Solving (50) for Δ,

$$\Delta=\left[1-\frac{1}{q\rho-1}\right]^{1/2}-1\,. \tag{51}$$

When $q\rho$ is large, we have $\Delta \approx -1/(2q\rho)$, or

$$d = -\rho\Delta \approx \frac{1}{2q} . \tag{52}$$

The defect distance is independent of the droplet radius for large droplets. Because we approximated the relaxed droplet as a circular section of an undeformed $s=2$ defect pattern, and assumed that the droplet remained centered on the $\hat{\mathbf{x}}$ axis, Eqs. (50)—(52) are probably good only to within factors of 2. However, d should not depend strongly on β, since F_2 varies only by factors of two over the allowed β's, so Eq. (50) allows the rough magnitude of the elastic constant q to be determined by direct observation of d. Examination of the droplets in Fig. 2 that q is roughly 140 ± 20 cm^{-1}. For the droplets in the photograph Eq. (52) is not valid, since $q\rho$ is only on the order of 4. If the stripe edge angle δ can be measured accurately, then Eq. (30) can then be used to find β, which determines the elastic constants up to the multiplicative factor K.

APPENDIX A: ENUMERATING THE SECOND-ORDER BULK GRADIENT TERMS

The most general second-order bulk gradient term is, as explained in Sec. II B 1,

$$F_2^\alpha = T^\alpha_{ijkl}(\partial_i c_j)(\partial_k c_l) . \tag{A1}$$

The tensors T^α_{ijkl} can be thought of as elements of a 16-dimensional vector space T. Each superscript α refers to a different vector, and the subscripts $i,j,k,l=1,2$ refer to the 16 components. On rotating the x-y coordinate system around $\hat{\mathbf{z}}$, the components of ∂ and $\hat{\mathbf{c}}$ transform according to the two-dimensional continuous rotation group C_∞ The vectors T^α_{ijkl} therefore transform according to the symmetrized direct-product group

$$G = (C_\infty \otimes C_\infty) \circledS (C_\infty \otimes C_\infty) , \tag{A2}$$

where $\otimes$ indicates a direct product and $\circledS$ indicates a symmetric direct product. The symmetric product is used because of the symmetry of T^α_{ijkl} under the simultaneous interchange of i with k and j with l. The form of F_2^α is unchanged by the rotation if and only if T^α_{ijkl} is invariant under the action of G.

The vector space T can be divided into a number of irreducible subspaces such that G maps each subspace into itself. These subspaces correspond to the irreducible representations of G.[14,15] The number of independent and invariant T^α_{ijkl}'s is equal to the number of n_1 of irreducible one-dimensional representations of G. n_1 is determined by analysis of the group characters.

The elements of the group C_∞ are

$$R(\theta) = \begin{bmatrix} \cos\theta & \sin\theta \\ -\sin\theta & \cos\theta \end{bmatrix} . \tag{A3}$$

The character χ of a representation of a group element is the trace of the corresponding matrix, so

$$\chi(R(\theta)) = 2\cos\theta . \tag{A4}$$

The character of a direct product is the product of the characters, but the character of a symmetric product of a group with itself is[16]

$$\chi(A \circledS A) = \tfrac{1}{2}\{[\chi(A)]^2 + \chi(A^2)\} . \tag{A5}$$

The characters of G are therefore

$$\chi(G) = \tfrac{1}{2}\{[\chi(C_\infty \otimes C_\infty)]^2 + \chi((C_\infty \otimes C_\infty)^2)\} , \tag{A6}$$

so

$$\chi(G(\theta)) = \tfrac{1}{2}[16\cos^4\theta + 4\cos^2(2\theta)] . \tag{A7}$$

The number of times an irreducible representation α appears in a finite group H is given by[15]

$$n_\alpha = \frac{1}{o(H)} \sum_{h \in H} \chi(h)\chi^\alpha(h)^* , \tag{A8}$$

where $o(H)$ is the number of elements in the group. Generalizing to continuous groups and setting $\chi^\alpha(h)=1$ (since the one-dimensional scalar representation has $\chi=1$) we have

$$n_1 = \frac{1}{2\pi}\int_0^{2\pi} \chi(G(\theta))d\theta , \tag{A9}$$

which implies that $n_1 = 4$.

Since δ_{ij} and ε_{ij} are rotationally invariant, we can immediately write down four invariant tensors,

$$T^1_{ijkl} = \delta_{ij}\delta_{kl} , \tag{A10a}$$

$$T^2_{ijkl} = \varepsilon_{ij}\varepsilon_{kl} , \tag{A10b}$$

$$T^3_{ijkl} = \tfrac{1}{2}(\delta_{ij}\varepsilon_{kl} + \varepsilon_{ij}\delta_{kl}) , \tag{A10c}$$

and

$$T^4_{ijkl} = \delta_{ik}\delta_{jl} , \tag{A10d}$$

which lead directly to the free-energy terms (3). The linear independence of these four tensors may be verified by inspection. Because $n_1=4$, these are the only possible independent tensors, and the second-order rotationally invariant bulk gradient terms are completely accounted for.

APPENDIX B: GRADIENTS AND SURFACE TERMS

In this appendix we demonstrate that the surface free-energy density $F_{\rm surf}$ cannot depend upon gradients of the order parameter to lowest order. We will describe the boundary in terms of local coordinates $\hat{\mathbf{n}}(x,y)$ and $\hat{\mathbf{l}}(x,y)$, where $\hat{\mathbf{n}}$ is normal to the boundary and $\hat{\mathbf{l}}$ is parallel to it and points counterclockwise. For convenience, we will define ϕ relative to $\hat{\mathbf{n}}$. This definition is unambiguous sufficiently close to the boundary. (See Fig. 12.)

First, a term in $F_{\rm surf}$ that is proportional to a derivative of ϕ normal to the boundary can diverge without affecting the value of the order parameter in the bulk or at the surface. Consider a film pattern $\phi(x,y)$ determined by minimizing F_2 with some imposed boundary condition. In a strip of width ϵ along the edge of the film, perturb the order-parameter field by setting

$$\frac{\partial\phi}{\partial n} = \epsilon^{-\gamma} . \tag{B1}$$

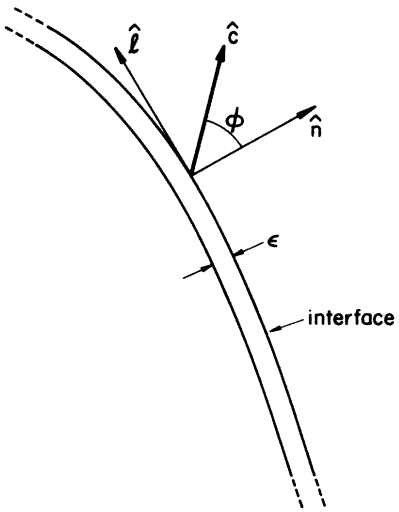

FIG. 12. Definition of the coordinate system for surface terms. Derivatives of ϕ with respect to $\hat{\mathbf{n}}$ diverges as $\epsilon \rightarrow 0$.

The change in the bulk free energy $\mathscr{F}_2$ due to this perturbation is of order

$$\Delta\mathscr{F}_2 \approx \int_0^{\epsilon} dn\,(\epsilon^{-\gamma})^2 \approx \epsilon^{1-2\gamma} \tag{B2}$$

and the change in ϕ at the boundary is of order

$$\Delta\phi_0 \approx \int_0^{\epsilon} dn\,\epsilon^{-\gamma} \approx \epsilon^{1-\gamma}\ . \tag{B3}$$

Now let $\epsilon \rightarrow 0$. If $0 < \gamma < \frac{1}{2}$, then $\Delta\phi_0 = 0$, so the boundary condition still holds, and $\Delta\mathscr{F}_2 = 0$, so the pattern still minimizes the bulk free energy, but the derivative $\partial\phi/\partial n$ diverges. Similar arguments hold for any derivative $\partial^m\phi/\partial n^m$. Hence, any term in F_{surf} which is proportional to a normal derivative of the order parameter can diverge and make the surface free energy negatively infinite, without affecting any bulk properties of the film. On the other hand, there is a physical limit to the size of any derivative. Derivatives of ϕ are not defined on a length scale smaller than the molecular length a, so mth derivatives should be set equal to a constant factor $\pm a^{-m}$. Since a term containing m derivatives is multiplied by an elastic constant that scales as a^m, the fact that a^{-m} diverges for large m is inconsequential. In fact, replacing all normal derivatives by a^{-m} and letting them cancel their elastic constants removes all dependence of F_{surf} on the normal derivatives.

This argument cannot be extended to cover derivatives of the order parameter with respect to position along the boundary, since $\partial\phi/\partial l$ cannot diverge in a narrow strip if ϕ is to be continuous everywhere in the bulk. Hence, F_{surf} *can* depend on tangential derivatives of $\hat{\mathbf{c}}$.

Because of rotational symmetry, F_{surf} can depend only upon $\hat{\mathbf{c}}$, $\hat{\mathbf{n}}$, and derivatives with respect to l. We will assume that the curvature of the boundary is small, so that derivatives of $\hat{\mathbf{n}}$ with respect to l can be ignored. Expanding F_{surf} in a Taylor series in l,

$$F_{\text{surf}} = f_0(\hat{\mathbf{c}},\hat{\mathbf{n}}) + \vec{f}_1(\hat{\mathbf{c}},\hat{\mathbf{n}})\cdot\frac{\partial\hat{\mathbf{c}}}{\partial l} + \cdots \tag{B4}$$

we wish to show that the first-order term cannot contribute to the free energy. $\vec{f}_1$ can be decomposed into components parallel and perpendicular to $\hat{\mathbf{c}}$,

$$[\vec{f}_1(\hat{\mathbf{c}},\hat{\mathbf{n}})]_i = f_{\parallel}(\hat{\mathbf{c}},\hat{\mathbf{n}})c_i + f_{\perp}(\hat{\mathbf{c}},\hat{\mathbf{n}})\varepsilon_{ij}c_j \tag{B5}$$

so that

$$\vec{f}_1(\hat{\mathbf{c}},\hat{\mathbf{n}})\cdot\frac{\partial\hat{\mathbf{c}}}{\partial l} = f_{\parallel}(\hat{\mathbf{c}},\hat{\mathbf{n}})\hat{\mathbf{c}}\cdot\frac{\partial\hat{\mathbf{c}}}{\partial l} + f_{\perp}(\hat{\mathbf{c}},\hat{\mathbf{n}})\hat{\mathbf{c}}\times\frac{\partial\hat{\mathbf{c}}}{\partial l}\ . \tag{B6}$$

The first term vanishes identically because $\hat{\mathbf{c}}$ is a unit vector. $\hat{\mathbf{c}}\times\partial\hat{\mathbf{c}}/\partial l$ is symmetric under 180° rotations about $\hat{\mathbf{x}}$, so $f_{\perp}(\hat{\mathbf{c}},\hat{\mathbf{n}})$ must also be symmetric. Section II B 2 shows that such a function of $\hat{\mathbf{c}}$ and $\hat{\mathbf{n}}$ can be written as a function of $\hat{\mathbf{c}}\times\hat{\mathbf{n}}$ alone. Expanding $f_{\perp}$ in powers of $\hat{\mathbf{c}}\times\hat{\mathbf{n}}$,

$$\vec{f}_1(\hat{\mathbf{c}},\hat{\mathbf{n}})\cdot\frac{\partial\hat{\mathbf{c}}}{\partial l} = \sum_k A_k^l(\hat{\mathbf{c}}\times\hat{\mathbf{n}})^k\hat{\mathbf{c}}\times\frac{\partial\hat{\mathbf{c}}}{\partial l} \tag{B7}$$

and noticing that $\hat{\mathbf{c}}\times\hat{\mathbf{n}} = -\sin\phi$ and $\hat{\mathbf{c}}\times(\partial\hat{\mathbf{c}}/\partial l) = \partial\phi/\partial l$, we find

$$\vec{f}_1(\hat{\mathbf{c}},\hat{\mathbf{n}})\cdot\frac{\partial\hat{\mathbf{c}}}{\partial l} = \sum_k A_k\sin^k\phi\frac{\partial\phi}{\partial l} = \frac{\partial}{\partial l}\sum_k A_k\frac{1}{k+1}\sin^{k+1}\phi\ , \tag{B8}$$

which is a total derivative. Therefore the net surface energy vanishes to first order in $\partial/\partial l$,

$$F_{\text{surf},1} = \oint dl\,\vec{f}_1(\hat{\mathbf{c}},\hat{\mathbf{n}})\cdot\frac{\partial\hat{\mathbf{c}}}{\partial l} = 0\ . \tag{B9}$$

In the presence of a singularity on the surface (as in Fig. 4), this term is a nonzero constant which merely renormalizes the defect core energy.

To lowest order, only second tangential derivatives may appear in the surface free-energy density. However, these derivatives are of order $1/R^2$, where R is the system size, so their contribution to $\mathscr{F}$ scales like a/R. The second-order surface terms are a factor of a/R smaller than the bulk terms in (10) and can be neglected, leaving F_{surf} free of derivatives.

ACKNOWLEDGMENTS

The authors wish to thank Noel Clark and David Van Winkle for bringing this problem to their attention. We thank Bob Pelcovits for helpful conversations. This work was supported by National Science Foundation Grant No. DMR-8451921.

[1]C. Y. Young, R. Pindak, N. A. Clark, and R. B. Meyer, Phys. Rev. Lett. **40**, 737 (1978).

[2]C. Rosenblatt, R. B. Meyer, R. Pindak, and N. A. Clark, Phys. Rev. A **21**, 140 (1980).

[3]R. Pindak, C. Y. Young, R. B. Meyer, and N. A. Clark, Phys. Rev. Lett. **45**, 1193 (1980).

[4]D. H. Van Winkle and N. A. Clark, Phys. Rev. Lett. **53**, 1157 (1984).

[5]P. G. de Gennes, *The Physics of Liquid Crystals* (Clarendon, Oxford, 1975), p. 125.

[6]N. A. Clark, D. H. Van Winkle, and C. Muzny (private communication).

[7]P. A. C. Gane, A. J. Leadbetter, J. J. Benattar, F. Moussa, and M. Lambert, Phys. Rev. A **24**, 2694 (1981); J. D. Brock, A. Aharony, R. J. Birgeneau, K. W. Evans-Lutterodt, J. D. Litster, P. M. Horn, G. B. Stephenson, and A. R. Tajbakhsh, Phys. Rev. Lett. **57**, 98 (1986). Unlike the material studied by Brock *et al.*, the Sm$C \rightarrow$SmI transition in HOBACPC is first order. It might seem that the type of translational order is not important to us, since our order parameter for SmI describes purely the orientational order. However, we also ignore thermal fluctuations in the orientational order; in principle, if the translational order in a film of HOBACPC in the SmI phase is short range, then the orientational order in the absence of an external field will decay algebraically with distance. There is no evidence of this decay on the length scale of the textures we study, although it could occur on longer lengthscales.

[8]P. G. de Gennes, *The Physics of Liquid Crystals* (Clarendon, Oxford, 1975), p. 319.

[9]Our derivation of the bulk free energy leads to the same terms found by de Gennes (Ref. 5) for a three-dimensional chiral SmC, if we ignore all terms involving the third dimension. Our surface term is more general, although, in the end, the only term we keep is identical to that of de Gennes.

[10]N. D. Mermin, in *Quantum Fluids and Solids*, edited by S. B. Trickey, E. Adams, and J. Duffy (Plenum, New York, 1977). N. David Mermin has confirmed that this is a natural extension of the term "boojum."

[11]C. R. Hu, T. E. Ham, and W. M. Saslow, J. Low Temp. Phys. **32**, 301 (1978).

[12]Actually, a point defect has a small but finite radius Λ, so the free-energy density does not diverge. Within the defect the liquid crystal is melted, at the cost of a core free energy. For sufficiently strong core energies and sufficiently small defect radii the $s=2$ boojum has a lower energy than the $s=1$ pattern shown in Fig. 8, because the boojum has no defect core. The definition of "sufficiently" depends upon the elastic constant β. For the special case $\beta=-1$ and $\phi_0=\pi/2$ the requirement is simply that $\Lambda<1/q$, since for these cases the leading terms in the free energy near the defect go as $2\pi K\ln(R/\Lambda)$ for $s=1$ and $2\pi K\ln(qR)$ for $s=2$.

[13]The droplet pattern is not in equilibrium, since the droplets grow and eventually transform into stripes. However, we can apply equilibrium methods if we assume that the internal relaxations of the order-parameter field are fast compared to the rate of growth of the droplet.

[14]M. Tinkham, *Group Theory and Quantum Mechanics* (McGraw Hill, New York, 1964).

[15]L. D. Landau and E. M. Lifshitz, *Quantum Mechanics (Non-relativistic Theory)*, Vol. 3 of *Course of Theoretical Physics* (Pergamon, New York, 1977), p. 368.

[16]The notation, though technically imprecise, is clear. When the argument of χ is a group, rather than a group element, the relation holds for all elements of the group.

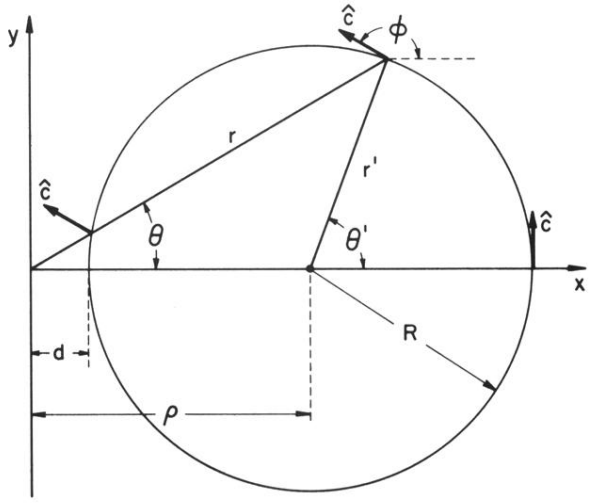

(a)

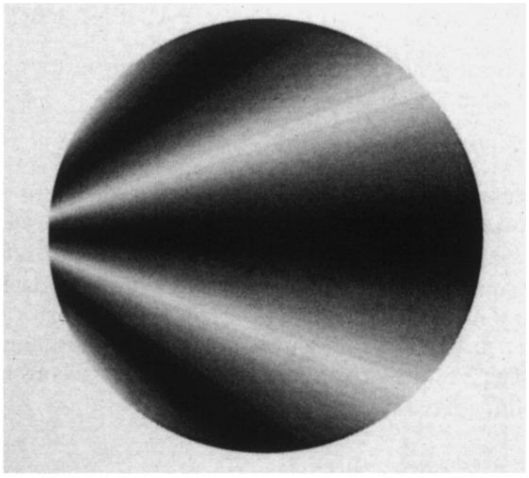

(b)

FIG. 11. (a) Geometry of the droplets. ϕ is a function only of θ. The droplet has moved a distance d relative to the defect. When $d=0$ the boundary conditions are met exactly, as in Fig. 4(a). (b) Computer generated *schlieren* pattern for the configuration of (a), with $d=R/4$.

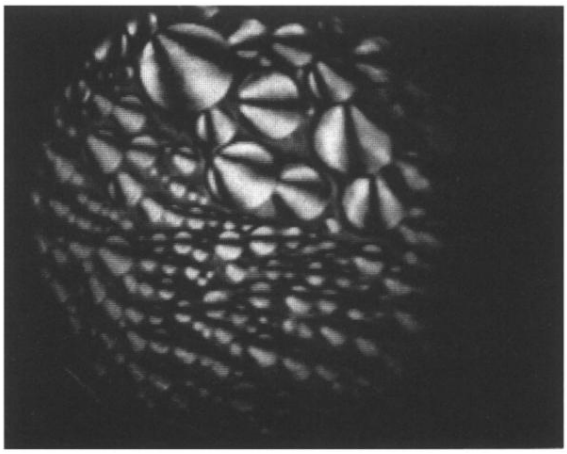

FIG. 2. Polarized reflection micrograph of the droplet texture. The polarization axes are parallel to the edges of the picture. The diameter of the illuminated region is roughly 0.24 cm. Photo courtesy of N. A. Clark, D. H. Van Winkle, and C. Muzny.

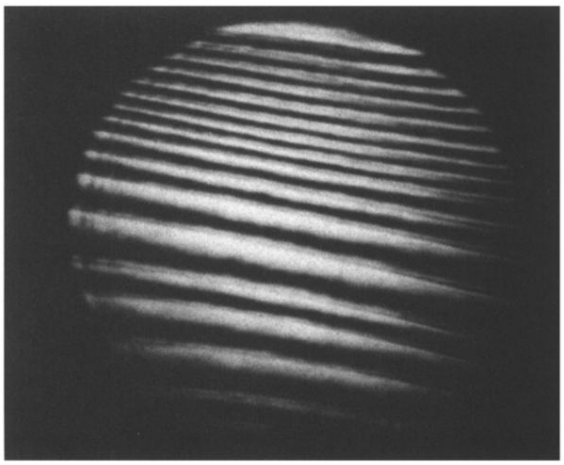

FIG. 3. Polarized reflection micrograph of the stripe texture. Photo courtesy of N. A. Clark, D. H. Van Winkle, and C. Muzny.

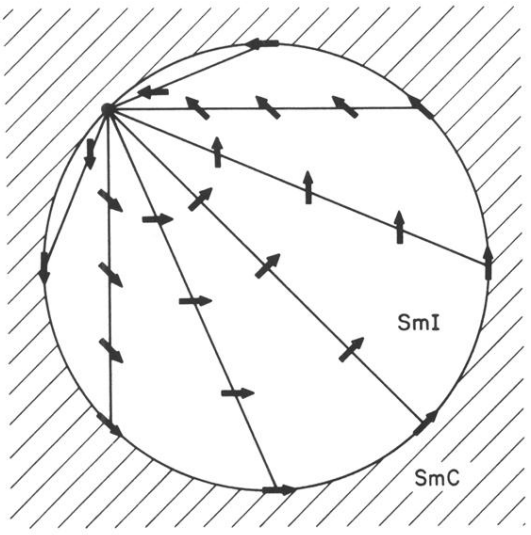

(a)

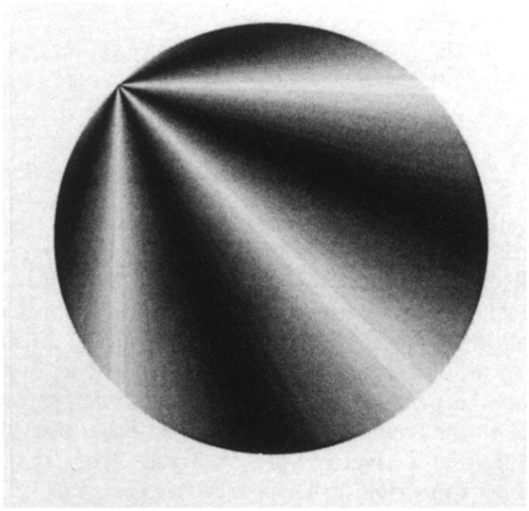

(b)

FIG. 4. (a) Texture within an ideal droplet. The order parameter is everywhere parallel to the boundary at the boundary, and the orientation of the order parameter is constant along any straight line passing through the defect point. (b) Computer-generated *schlieren* pattern for the configuration of (a).